Dichotomous-noise-induced pattern formation in a reaction-diffusion system

Debojyoti Das and Deb Shankar Ray*
Indian Association for the Cultivation of Science, Jadavpur, Kolkata 700 032, India
(Received 30 January 2013; revised manuscript received 24 April 2013; published 27 June 2013)

We consider a generic reaction-diffusion system in which one of the parameters is subjected to dichotomous noise by controlling the flow of one of the reacting species in a continuous-flow-stirred-tank reactor (CSTR) -membrane reactor. The linear stability analysis in an extended phase space is carried out by invoking Furutzu-Novikov procedure for exponentially correlated multiplicative noise to derive the instability condition in the plane of the noise parameters (correlation time and strength of the noise). We demonstrate that depending on the correlation time an optimal strength of noise governs the self-organization. Our theoretical analysis is corroborated by numerical simulations on pattern formation in a chlorine-dioxide-iodine-malonic acid reaction-diffusion system.

DOI: 10.1103/PhysRevE.87.062924 PACS number(s): 89.75.Kd, 82.40.Bj, 82.40.Ck

I. INTRODUCTION

Noise is ubiquitous in natural sciences. While traditionally noise acts as an impediment for order, signal, or communication networks, its constructive role has attracted a lot of attention over the last three decades [1,2]. A closer look reveals two distinct situations in zero-dimensional systems. First, noise may assist activation so that a multistable system can cross a potential barrier and the barrier crossing rate becomes maximum at an optimal noise strength. Stochastic resonance [3] and several of its variants such as resonant activation [4], coherence resonance [5], and ratchets [6] fall in this category. In the second case noise may destabilize a steady state while inducing creation of new steady states [7]. Examples include, among others, noise-induced nonequilibrium transition [7,8], flashing ratchet [9], and Parrondo's paradox [10]. When the system is spatially extended as in reaction-diffusion systems, the local kinetics gets diffusively coupled and the scenario encompasses a broader area covering noise-induced pattern formation. This occurs when an external spatially and temporally uncorrelated noise in a system parameter induces a patterned state which otherwise remains homogeneously stable in the absence of fluctuations [2]. The effects of additive as well as multiplicative noise have been explored [11] in various reaction-diffusion systems, electrodynamic convection in nematic liquid crystals, the Swift-Hohenberg model for turbulence, and in many other issues. The scope of techniques ranges from mean-field approximation [2,12], Langevin-Fokker-Planck hybrid description [13], and higher order moment approach [14] to renormalization-group methods [2,15]. For a comprehensive review we refer to Sagués *et al.* [2].

The focus of the present work is pattern formation induced by dichotomous noise. The problem has been addressed previously by several groups [16–23]. For example, the switching triggered by dichotomous fluctuations results in an interplay of two different dynamics, neither of which supports a patterned state, leading to the formation of Turing patterns. Turing pattern formation has also been investigated in the presence of additive dichotomous noise in diffusively coupled FitzHugh-Nagumo kinetics [20] for various switching rates. The major emphasis of these studies lies on a switching mechanism [16–20] that leads to self-organization. Furthermore, most of the investigations on noise-induced pattern formation are based on white noise. For a noise process whose time scale is much faster compared to the time scale of the deterministic part of the dynamical system, a white-noise limit serves as a good approximation. On the other hand, when the two time scales are close to each other one has to go beyond this limit and resort to appropriate noise correlation. The question is, how does the interplay of the correlation time and the strength of the dichotomous fluctuations govern self-organization in a reaction-diffusion system? The physical motivation here stems from consideration of the following situation. We maintain the reaction-diffusion system under study in a CSTR-membrane reactor [also called a continuous-flow-unstirred reactor (CFUR)] [24] in which the flow of one of the species (whose concentration is kept large such that it can be treated approximately as a constant in the absence of any fluctuation) can be subjected to stochastic fluctuations. Such stochastic modulation of concentration of a substrate in a chemical reaction in a continuous-flow-stirred-tank reactor is well known, for example, in glycolysis [25]. Our aim is to look for the bifurcation condition for dichotomous-noise-induced instability in this reaction-diffusion system. For a dichotomous noise with zero mean and Ornstein-Zernike correlator we derive here the critical line in the σ-λ parameter plane, where σ and λ refer to the noise strength and inverse of correlation time, respectively. The instability condition is examined in a prototypical chemical reaction-diffusion system (chlorine-dioxide-iodine-malonic acid system [26–33]) which has served as an excellent testing ground for various theories of pattern formation and related contexts. We show that depending on the correlation time, an optimal range of noise strength is necessary for noise-induced self-organization or stationary pattern formation. Our theoretical scheme has been corroborated by detailed numerical simulation on this system.

The paper is organized as follows: In Sec. II we introduce a two-component reaction-diffusion system in which one of the parameters is subjected to dichotomous fluctuations.

*Email address: pcdsr@iacs.res.in

The instability condition is derived in the noise-strength–correlation-time parameter space to distinguish between the homogeneous and the inhomogeneous regimes. The theoretical formulation is illustrated in Sec. III in the light of the chlorine-dioxide-iodine-malonic acid reaction-diffusion system and its numerical simulations. The paper is concluded in Sec. IV.

II. THE TWO-COMPONENT MODEL AND DICHOTOMOUS-NOISE-INDUCED INSTABILITY: GENERAL SCHEME

We consider a general two-component reaction-diffusion system characterized by parameters p_U and p_V (e.g., rate constants or concentrations of the species treated as constants, etc.) corresponding to two species with concentration U and V that react and diffuse as follows:

$$\frac{\partial U}{\partial t} = F(U,V,p_U) + \nabla^2 U, \qquad \frac{\partial V}{\partial t} = G(U,V,p_V) + d\nabla^2 V, \tag{2.1}$$

where $U(x,y,t)$ and $V(x,y,t)$, the concentration variables, are functions of space and time. $F(U,V,p_U)$ and $G(U,V,p_V)$ express the local reaction kinetics in terms of the functional dependence on the variables and parameters. d denotes the ratio of diffusion coefficients of the two species. We assume that the system admits a homogeneous steady state at concentrations U_0 and V_0 such that

$$F(U_0,V_0,p_U) = 0, \quad G(U_0,V_0,p_V) = 0. \tag{2.2}$$

Applying linear perturbation analysis about the steady state ($U = U_0 + \bar{u}, V = V_0 + \bar{v}$), where the spatial perturbation can be expressed as $\bar{u} = u(t)\cos(k_x x)\cos(k_y y)$ and $\bar{v} = v(t)\cos(k_x x)\cos(k_y y)$, we obtain

$$\frac{\partial u}{\partial t} = Pu + Qv, \qquad \frac{\partial v}{\partial t} = R_1 u + S_1 v. \tag{2.3}$$

Here $P = [F_U - (k_x^2 + k_y^2)]$, $Q = F_V$, $R_1 = G_U$, and $S_1 = [G_V - d(k_x^2 + k_y^2)]$. F_U, F_V, G_U, and G_V are the respective partial derivatives of the functions $F(U,V)$ and $G(U,V)$ with respect to U and V. k_x and k_y are the wave-vector components along the x and y directions. We further assume that the homogeneous steady state is linearly stable with respect to spatially homogeneous perturbations, i.e., stable in the absence of diffusion. This requires that the sufficient conditions are given by

$$F_U + G_V < 0, \quad F_U G_V - F_V G_U > 0. \tag{2.4}$$

Introduction of diffusion, on the other hand, yields the Turing condition, i.e., the homogeneous steady state loses its stability with respect to spatiotemporal perturbation if the following condition holds good:

$$\frac{[dF_U + G_V]^2}{4d} > F_U G_V - F_V G_U. \tag{2.5}$$

We now consider that one of the parameters, say, p_V, is perturbed by fluctuation or noise, i.e., $p_V = p_0 + \xi(t)$, where p_0 is the constant part and $\xi(t)$ denotes a dichotomous noise with zero mean and Ornstein-Zernike correlator,

$$\langle \xi(t) \rangle = 0, \quad \langle \xi(t)\xi(t') \rangle = \sigma \exp(-\lambda |t - t'|). \tag{2.6}$$

Physically, this may be achieved by stochastic variation of the concentration of one of the species (which is large compared to u or v in the absence of fluctuation) included in p_V when the reaction is carried out in a CSTR-membrane reactor [24]. Therefore, Eqs. (2.3) with multiplicative noise take the following form:

$$\frac{\partial u}{\partial t} = Pu + Qv, \qquad \frac{\partial v}{\partial t} = Ru + \theta_1 \xi u + Sv + \theta_2 \xi. \tag{2.7}$$

Here θ_1 and θ_2 are the parts of G_U and G_V without p_0, respectively, and R and S refer to the parts of G_U and G_V with p_0, respectively. Eqs. (2.7) on averaging, take the form

$$\frac{\partial \langle u \rangle}{\partial t} = P\langle u \rangle + Q\langle v \rangle, \qquad \frac{\partial \langle v \rangle}{\partial t} = R\langle u \rangle + \theta_1 \langle \xi u \rangle + S\langle v \rangle + \theta_2 \langle \xi v \rangle. \tag{2.8}$$

To proceed further we need the correlators $\langle \xi u \rangle$ and $\langle \xi v \rangle$. They can be dealt with using the Furutzu-Novikov [34] procedure, which, for exponentially correlated random function [Eq. (2.6)] takes the Shapiro-Logunov [35] form, viz.,

$$\frac{d\langle \xi u \rangle}{\partial t} = \left\langle \xi \frac{du}{dt} \right\rangle - \lambda \langle \xi u \rangle, \qquad \frac{d\langle \xi v \rangle}{\partial t} = \left\langle \xi \frac{dv}{dt} \right\rangle - \lambda \langle \xi v \rangle. \tag{2.9}$$

On multiplying Eqs. (2.7) by ξ, and subsequent averaging, one obtains

$$\left\langle \xi \frac{du}{dt} \right\rangle = P\langle \xi u \rangle + Q\langle \xi v \rangle, \qquad \left\langle \xi \frac{dv}{dt} \right\rangle = R\langle \xi u \rangle + S\langle \xi v \rangle + \theta_1 \langle \xi^2 u \rangle + \theta_2 \langle \xi^2 v \rangle. \tag{2.10}$$

To get around the higher-order correlators $\langle \xi^2 u \rangle$ and $\langle \xi^2 v \rangle$ in Eqs. (2.10), one, in general, may resort to decoupling approximations. However, we make use of the special case of the two-state Markov process (dichotomous noise) which is described by the correlator (2.6) and $\xi^2 = \sigma$. Consequently, Eqs. (2.9) take the following form:

$$\frac{d\langle \xi u \rangle}{\partial t} = P\langle \xi u \rangle + Q\langle \xi v \rangle - \lambda \langle \xi u \rangle, \qquad \frac{d\langle \xi v \rangle}{\partial t} = \sigma[\theta_1 \langle u \rangle + \theta_2 \langle v \rangle] + R\langle \xi u \rangle + [S - \lambda]\langle \xi v \rangle. \tag{2.11}$$

Equations (2.8) and (2.11) constitute a closed set of linear equations for four coupled variables $\langle u \rangle$, $\langle v \rangle$, $\langle \xi u \rangle$, and $\langle \xi v \rangle$. We emphasize that because of the appearance of the additional variables $\langle \xi u \rangle$ and $\langle \xi v \rangle$ the phase space for the linear analysis is now extended [36]. Assuming solutions of the form $\langle u \rangle = \langle \bar{u} \rangle e^{-\epsilon t}$, $\langle v \rangle = \langle \bar{v} \rangle e^{-\epsilon t}$, $\langle \xi u \rangle = \langle \bar{\xi u} \rangle e^{-\epsilon t}$, and $\langle \xi v \rangle = \langle \bar{\xi v} \rangle e^{-\epsilon t}$ for each of the four variables and substituting them in Eqs. (2.8) and (2.11), we obtain the following equation for the determinant, $|\epsilon I - M| = 0$, where

$$M = \begin{bmatrix} P & Q & 0 & 0 \\ R & S & \theta_1 & \theta_2 \\ 0 & 0 & P-\lambda & Q \\ \sigma\theta_1 & \sigma\theta_2 & R & S-\lambda \end{bmatrix}. \tag{2.12}$$

I is the identity matrix, ϵ is the eigenvalue to be determined, and M is the stability matrix in the extended phase space. Expansion of the above determinant gives

$$\begin{aligned}&\epsilon^4 - 2(P+S-\lambda)\epsilon^3 + \{P(P+2S-2\lambda) + S(P+S-2\lambda) + \lambda^2 - (P+S)\lambda + PS - 2RQ - \sigma\theta_2^2\}\epsilon^2\\ &+\{P[S(P+S-2\lambda) + \lambda^2 - (P+S)\lambda + PS - RQ - \sigma\theta_2^2] + S[\lambda^2 - (P+S)\lambda + PS - RQ]\\ &+\sigma\theta_1\theta_2 Q - \sigma\theta_2^2(P-\lambda) - Q[R(P+S-2\lambda) - \sigma\theta_1\theta_2]\}\epsilon + PS[\lambda^2 - (P+S)\lambda + PS - RQ] + \sigma\theta_1\theta_2 PQ\\ &-\sigma\theta_2^2(P-\lambda)P - Q\{R[\lambda^2 - (P+S)\lambda + PS - RQ] + \sigma\theta_1^2 Q - \sigma\theta_1\theta_2(P-\lambda)\} = 0.\end{aligned} \tag{2.13}$$

We now invoke the Routh-Hurwitz stability criterion [37] for the characteristic equation

$$|\epsilon I - M| = \epsilon^4 + B_1\epsilon^3 + B_2\epsilon^2 + B_3\epsilon + B_4 = 0, \tag{2.14}$$

where B_1, B_2, B_3, and B_4 can be directly identified from the coefficients of the powers of ϵ in Eq. (2.13). The eigenvalues ϵ of the 4×4 square matrix M, have all negative real parts, if $\Delta_1 > 0$, $\Delta_2 > 0$, $\Delta_3 > 0$, and $\Delta_4 > 0$ where, in general, Δ_k is given by

$$\Delta_k = \begin{vmatrix} B_1 & 1 & 0 & 0 & 0 & 0 & \cdots & 0 \\ B_3 & B_2 & B_1 & 1 & 0 & 0 & \cdots & 0 \\ B_5 & B_4 & B_3 & B_2 & B_1 & 1 & \cdots & 0 \\ \vdots & \vdots & \vdots & \vdots & \vdots & \vdots & \ddots & \vdots \\ B_{2k-1} & B_{2k-2} & B_{2k-3} & B_{2k-4} & B_{2k-5} & B_{2k-6} & \cdots & B_k \end{vmatrix}. \tag{2.15}$$

The system looses its stability if at least one of the Δ_k's becomes negative. A reasonable estimate of the critical values of correlation time ($\tau_c = 1/\lambda_c$) and strength (σ_c) of the dichotomous noise accompanying such a change in stability can be made by setting $\Delta_k = 0$ (here $k = 1, \ldots ,4$). Successive use of the associated relations yields the critical condition for instability for a given set of system parameters, which can be written in the following form:

$$\sigma_c = f(\lambda_c). \tag{2.16}$$

The actual form of $f(\lambda_c)$ varies from system to system. The critical σ_c-λ_c curve depicts a bifurcation scenario for noise-induced instability. Our scheme is the following: First, we select an appropriate homogeneous stable steady state of the system in the absence of noise outside the Turing domain. Second, the parameter space for this chosen state has to be used as an input to the stability matrix (M). Consequently the coefficients of the characteristic equation B_i,$i = 1,2,3,4,5,6,7$ are obtained. By varying the strength (σ_c) of the dichotomous noise as a function of correlation time (τ_c) or its inverse λ_c one can select the appropriate region in the σ_c-λ_c plane between the homogeneous state (in the presence of noise) and the patterned state. We now illustrate the procedure with the help of the following example.

III. APPLICATION

A. Chlorine-dioxide-iodine-malonic acid system

As an example, we consider the chlorine-dioxide-iodine-malonic acid(CDIMA) system [26–33], which is one of the most widely used paradigms for studying spatiotemporal patterns both numerically and experimentally over the last decade. Five key species are involved in the chemical reaction, viz., malonic acid (MA), I_2, ClO_2, I^-, and $ClO_2{}^-$ obeying the following chemical reactions:

$$\begin{aligned} MA + I_2 &\longrightarrow IMA + I^- + H^+,\\ ClO_2 + I^- &\longrightarrow ClO_2{}^- + \tfrac{1}{2}I_2,\\ ClO_2{}^- + 4I^- + 4H^+ &\longrightarrow Cl^- + 2I_2 + 2H_2O.\end{aligned} \tag{3.1}$$

An additional equilibrium between starch (S) and iodide ions occurs on adding starch from outside in the reaction medium (K being the equilibrium constant),

$$S + I^- + I_2 \rightleftharpoons SI_3{}^-, \quad K = \frac{[SI_3{}^-]}{[S][I^-][I_2]}. \tag{3.2}$$

Assuming the concentrations of malonic acid, chlorine dioxide, and iodine to remain practically constant and identifying U and V as the dimensionless concentrations of I^- and $ClO_2{}^-$, respectively, one can write the reduced two-variable model due to Lengeyl and Epstein [26], as follows:

$$\begin{aligned}\frac{\partial U}{\partial t} &= F(U,V) + \nabla^2 U,\\ \frac{\partial V}{\partial t} &= G(U,V) + cd\nabla^2 V.\end{aligned} \tag{3.3}$$

Here F and G can be identified as follows:

$$\begin{aligned}F(U,V) &= a - U - \frac{4UV}{1+U^2},\\ G(U,V) &= c\left[b\left(U - \frac{UV}{1+U^2}\right)\right].\end{aligned} \tag{3.4}$$

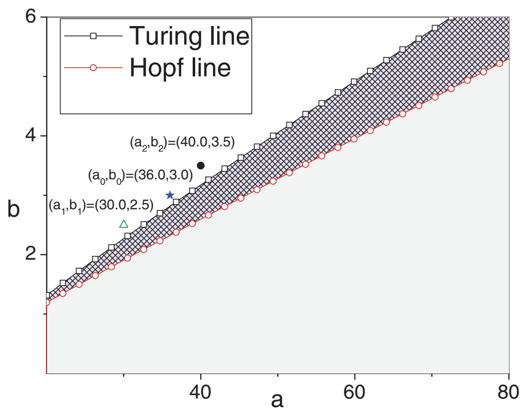

FIG. 1. (Color online) Bifurcation diagram for the CDIMA system without noise. The Turing line (square blocks) and the Hopf line (circles) are shown in the a-b parameter space. The shaded area in between the Turing and the Hopf line is the Turing region. Below the Hopf line lies the region for homogeneous oscillations. The region above the Turing line refers to homogeneous stable states. Three such states are shown by three points: ★, $(a_0,b_0) = (36.0,3.0)$); △, $(a_1,b_1) = (30.0,2.5)$; and •, $(a_2,b_2) = (40.0,3.5)$.

The parameters a and b are proportional to the concentration ratios $[\mathrm{MA}]/[\mathrm{I_2}]$ and $[\mathrm{ClO_2}]/[\mathrm{I_2}]$, respectively, and are related to kinetic parameters. d refers to the ratio of the diffusion coefficients $d = [\mathrm{D_{ClO_2^-}}]/[\mathrm{D_{I^-}}]$. c is the dimensionless concentration of starch which forms a complex with I^- such that $c = 1 + \mathrm{K[S]}$, where [S] is the concentration of starch. In order to bring the discussions into the present perspective we now consider the bifurcation diagram for the model CDIMA reaction as shown in Fig. 1. From the linear stability analysis it is well known that a Turing bifurcation curve is given by

$$(3a^2d - 5ab - 125d)^2 = 100abd(25 + a^2). \qquad (3.5)$$

This curve as depicted by the line on the a-b plane with square blocks in Fig. 1 for $d = 1.20$ is independent of c. The homogeneous steady state below it turns out to be unstable to inhomogeneous perturbation, i.e., to diffusion. The Hopf curve, on the other hand, is given by

$$bc = \frac{3a}{5} - \frac{25}{a}. \qquad (3.6)$$

Below this curve one observes homogeneous oscillations. By changing the concentration of the complexing agent, i.e., by varying c, it is possible to move the Hopf curve up or down in the a-b plane. A representative Hopf curve is shown in Fig. 1. by a solid line with circles for $c = 9.0$. When the Hopf curve lies below the Turing line, the Turing patterns arise in the shaded region below the Turing curve and above the Hopf curve. For further details we refer to [26–33].

B. Parametric dichotomous noise: Critical condition for noise-induced instability

In order to explore noise-induced instability it is necessary to select a point in the a-b stability diagram which corresponds to a homogeneous stable steady state (in the absence of noise). Three such representative states in Fig. 1 are denoted by the three points (a_0,b_0), (a_1,b_1), and (a_2,b_2) which lie above the Turing line, i.e., outside the shaded area of the normal Turing pattern. We then introduce the dichotomous noise in one of the kinetic parameters, i.e., $b = b_0 + \xi(t)$, where $\xi(t)$ is described fully by Eqs. (2.6) and set $a = a_0$. Following the scheme described in Sec. II, we obtain the set of four linear coupled equations [Eqs. (2.8) and (2.11)] for the CDIMA model when the dichotomous noise is switched on. Explicit calculation yields the quantities P, Q, R, S, θ_1, and θ_2 which are given as follows:

$$P = \left[\frac{3a_0^2 - 125}{a_0^2 + 25} - \left(k_x^2 + k_y^2\right)\right], \quad Q = -\left[\frac{20a_0}{a_0^2 + 25}\right],$$
$$R = \left[\frac{2a_0^2 b_0 c}{a_0^2 + 25}\right], \quad S = -\left[\frac{5a_0 b_0 c}{a_0^2 + 25} + cd\left(k_x^2 + k_y^2\right)\right], \qquad (3.7)$$
$$\theta_1 = \left[\frac{2a_0^2 c}{a_0^2 + 25}\right], \quad \theta_2 = -\left[\frac{5a_0 c}{a_0^2 + 25}\right].$$

As before, we obtain a quartic equation in ϵ, Eq. (2.13), with P, Q, R, S, θ_1, and θ_2 as defined above. For the CDIMA system, the coefficients $B_i, i = 1,2,3,4,5,6,7$ of Eq. (2.14) reduce to the following expressions:

$$\begin{aligned}
B_1 &= -2(P + S - \lambda),\\
B_2 &= \lambda^2 - 3(P + S)\lambda + 2(PS - RQ) + (P + S)^2 - \sigma\theta_2^2,\\
B_3 &= -\{(P + S)[\lambda^2 - (P + S)\lambda + PS - RQ]\\
&\quad + (PS - RQ)(P + S - 2\lambda) - 2\sigma\theta_1\theta_2 Q\\
&\quad - \sigma\theta_2^2(2P - \lambda)\},\\
B_4 &= (PS - RQ)[\lambda^2 - (P + S)\lambda + PS - RQ]\\
&\quad - \sigma\theta_1\theta_2(2P - \lambda)Q - \sigma\theta_2^2(P - \lambda) - \sigma\theta_1^2 Q^2,\\
B_5 &= 0, \quad B_6 = 0, \quad B_7 = 0.
\end{aligned} \qquad (3.8)$$

The corresponding Routh-Hurwitz coefficient Δ_k's are

$$\Delta_1 = |B_1|. \quad \Delta_2 = \begin{vmatrix} B_1 & 1 \\ B_3 & B_2 \end{vmatrix},$$
$$\Delta_3 = \begin{vmatrix} B_1 & 1 & 0 \\ B_3 & B_2 & B_1 \\ 0 & B_4 & B_3 \end{vmatrix}, \quad \Delta_4 = \begin{vmatrix} B_1 & 1 & 0 & 0 \\ B_3 & B_2 & B_1 & 1 \\ 0 & B_4 & B_3 & B_2 \\ 0 & 0 & 0 & B_4 \end{vmatrix}. \qquad (3.9)$$

The critical values of λ and σ are obtained by setting

$$\begin{aligned}
\Delta_1 &= B_1 = 0,\\
\Delta_2 &= B_1B_2 - B_3 = 0,\\
\Delta_3 &= B_1B_2B_3 - B_1^2B_4 - B_3^2 = 0,\\
\Delta_4 &= B_1B_2B_3B_4 - B_1^2B_4^2 - B_3^2B_4 = 0.
\end{aligned} \qquad (3.10)$$

$\Delta_1 = 0$ gives unphysical λ (hence unacceptable τ). Using the remaining equations, we obtain a quadratic equation in λ:

$$(PS - RQ)\lambda^2 - [(P + S)(PS - RQ) - \sigma\theta_2(\theta_1 Q + \theta_2 P)]\lambda + (PS - RQ)^2 - 2\sigma\theta_1\theta_2 PQ - \sigma\left[\theta_2^2P^2 + \theta_1^2Q^2\right] = 0. \qquad (3.11)$$

Considering small but finite correlation time τ (i.e., large λ), and thus retaining only the highest power of λ, we obtain the critical line $\sigma_c = f(\lambda_c)$ [see Eq. (2.16)] in the following form:

$$\sigma_c = \frac{(PS - RQ)\lambda_c^2 + (PS - RQ)^2}{\left[2\theta_1\theta_2 PQ + \theta_2^2 P^2 + \theta_1^2 Q^2\right]}. \qquad (3.12)$$

The critical bifurcation curve is given by Eq. (3.12). The region above this critical line corresponds to the homogeneous steady state in the presence of noise, while below it refers to the noise-induced patterned state. To realize the dichotomous-noise-induced spatiotemporal instability as given by the condition (3.12) we first depict the critical bifurcation line in the λ_c-σ_c plane. To draw this line we choose the homogeneous stable state above the Turing line in the absence of noise corresponding to the point $(a_0,b_0) = (36.0,3.0)$. The other parameters are set as $c = 9.0$ and $d = 1.20$. σ_c is calculated as a function of $\lambda_c(=\frac{1}{\tau_c})$ and the resulting critical line is shown in Fig. 2(a) by solid stars. The other two bifurcation lines are drawn and shown in the figure for the states $(a_1,b_1) = (30.0,2.5)$ and $(a_2,b_2) = (40.0,3.5)$; parameters c and d are kept the same. We conclude this section with a comment. Care must be taken to distinguish between two kinds of homogeneous states: one corresponding to the region above the Turing line in Fig. 1 where noise has no role to play with and the other corresponding to the region above the bifurcation line in the σ_c-λ_c plane. They are distinct because of dynamical considerations.

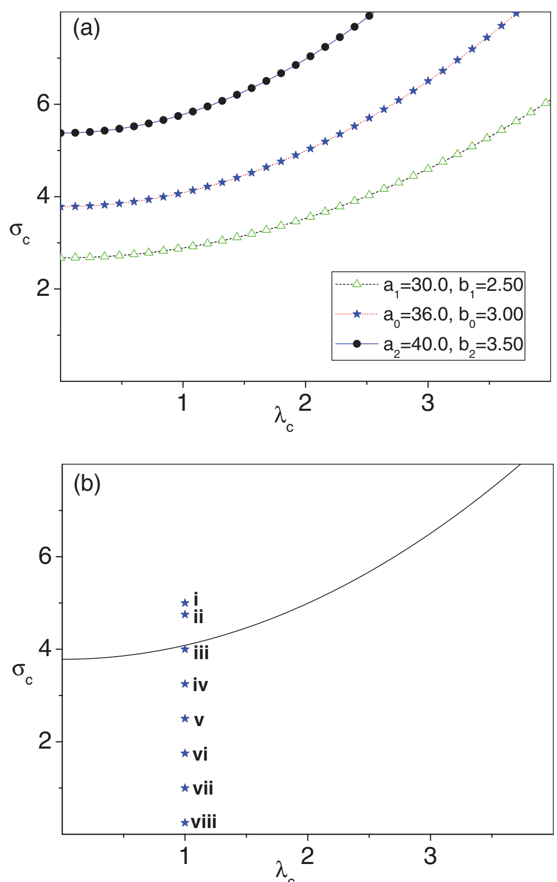

FIG. 2. (Color online) (a) Critical bifurcation curves [see Eq. (3.12)] for noise-induced instability for three different homogeneous stable states (in the absence of noise) shown in Fig. 1 for $c = 9.0$ and $d = 1.20$. (b) Critical bifurcation curve [see Eq. (3.12)] for dichotomous-noise-induced instability for the state $(a_0,b_0) = (36.0,3.00)$ (homogeneous stable in the absence of noise) with $c = 9.0$ and $d = 1.20$. The region above the line corresponds to homogeneous states in the presence of noise (representative points i and ii), while below it corresponds to the noise-induced patterned state (representative points iii–viii).

C. Numerical simulations: Noise-induced patterns

Since the critical line clearly makes a separation between the spatiotemporally stable and unstable regions, we choose several points (i, ii, iii, iv, v, vi, vii, and viii) in Fig. 2(b) in the parameter space on both sides of the line [drawn for the homogeneous stable state $(a_0,b_0) = (36.0,3.0)$ in the absence of noise] to carry out numerical simulations of Eqs. (3.3) with $a = a_0$ and $b = b_0 + \xi(t)$. Here $\xi(t)$ is the dichotomous noise with statistical properties given by Eq. (2.6). The numerical algorithm followed for generation of dichotomous noise with exponential correlation is given in Ref. [38]. The dichotomous noise $\xi(t)$ which can assume only two random values, say, α and β, constitute a random number sequence satisfying (2.6). Fig. 3(a) shows the illustrative dichotomous noise profiles for $\alpha = 1$ and $\beta = -1$ for three different values of correlation time τ. We emphasize that the time interval Δt between the two states is much smaller than τ $(\Delta t \ll \tau)$. It is clear from the figures that with an increase in correlation time, the residence time of a particular state increases on an average. The numerical accuracy of the method is checked by calculating the first moment $\langle \xi(t) \rangle$. In Fig. 3(b) we calculate the normalized

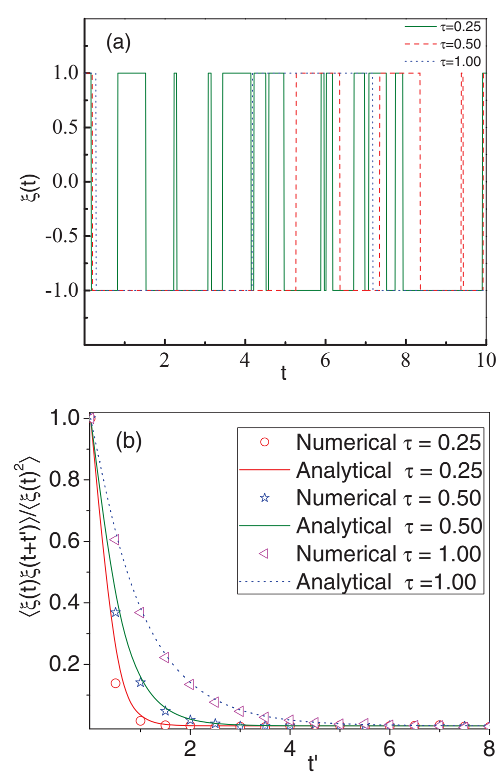

FIG. 3. (Color online) (a) Dichotomous noise profiles for two states $\alpha = 1$ and $\beta = -1$, for three different τ values. (b) Plots of the normalized correlation function versus t' for $\alpha = 1.0$ and $\beta = -1.0$, for three different noise profiles.

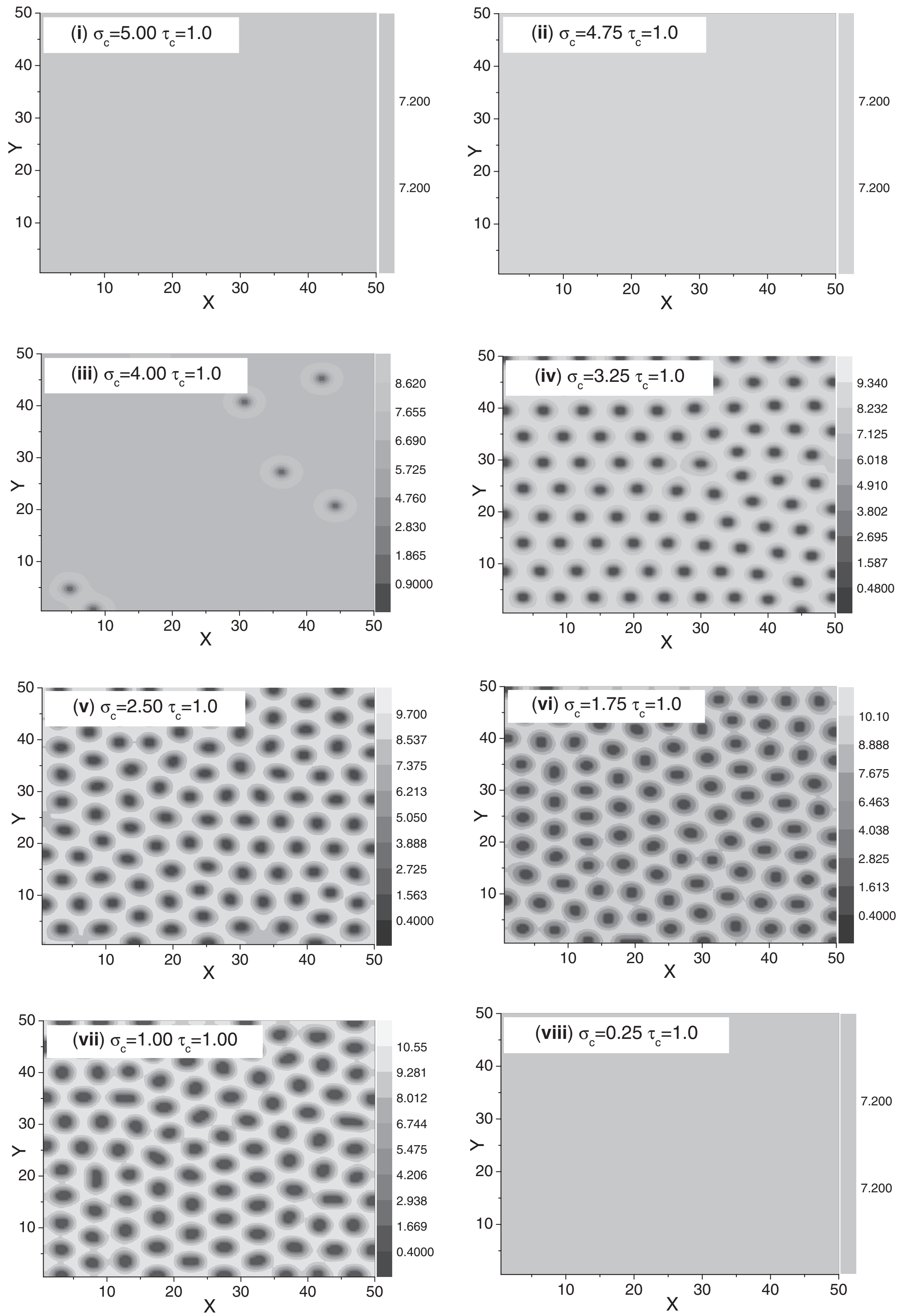

FIG. 4. Dichotomous-noise-induced stationary patterns for the parameter set $a = 36.0$, $b = 3.00$, $c = 9.0$, and $d = 1.20$ for various values of σ_c at a fixed $\tau_c = 1.0$. σ_c and τ_c values chosen for each figure correspond to each point in the parameter space of Fig. 2(b). (i) $\sigma_c = 5.00$, (ii) $\sigma_c = 4.75$, (iii) $\sigma_c = 4.00$, (iv) $\sigma_c = 3.25$, (v) $\sigma_c = 2.50$, (vi) $\sigma_c = 1.75$, (vii) $\sigma_c = 1.00$, and (viii) $\sigma_c = 0.25$. System size: 50×50 space units.

autocorrelation function $\langle \xi(t)\xi(t+t')\rangle/\langle \xi(t)^2\rangle$ corresponding to the noise profiles shown in Fig. 3(a).

Having generated the exponentially correlated dichotomous noise processes we are now in a position to explore noise-induced instability and pattern formation. The numerical simulation of Eq. (3.3) is done in two dimensions using the explicit Euler method. The computations have been performed on a 100×100 array with grid spacing $\Delta x = \Delta y = 0.50$ and a time step $\Delta t = 0.0025$ using a zero-flux boundary condition for the states represented by the points i, ii, iii, iv, v, vi, vii, and viii of Fig. 2(b) for a range of noise strength σ_c keeping τ_c fixed. The parameter set chosen is $(a_0,b_0) = (36.0,3.0)$ representing a homogeneous stable steady state in the a-b plane in the absence of noise (Fig. 1) with $c = 9.0$ and $d = 1.20$. With gradual lowering of noise strength σ_c as one approaches the bifurcation line from above no pattern appears for noise strength σ_c above the critical curve as shown in Figs. 4(i) and 4(ii). Instability sets in when the noise strength σ_c lies on the bifurcation curve. This is characterized by the appearance of precursors for the patterned state as shown in Fig. 4(iii). On further lowering of σ_c when the system is well below the bifurcation line the fully developed patterns appear for a range of noise strength. These are shown in Figs. 4(iv)–4(vii). The simulations are performed from a homogeneous state to an inhomogeneous patterned state, each state being considered after the system reaches the stationarity. The typical time to attain steady state is 4×10^5 time units. With further diminishing of the noise strength the pattern disappears [Fig. 4(viii)]. In order to corroborate this lack of patterns for very weak noise with our theoretical scheme we now return to the critical condition, Eq. (3.12). A closer look into this condition clearly suggests that as

$$\sigma_c \to 0, \quad \lambda_c^2 \to -(PS - RQ).$$

Explicit evaluation of P, Q, R, and S from Eq. (3.7) shows that $(PS - RQ)$ is positive for the parameter set chosen and therefore λ_c turns out to be purely imaginary. This implies that patterns cannot form at very low noise strength σ_c as observed in the numerical simulation shown in Fig. 4(viii).

We now explore the possible mechanism behind the dichotomous-noise-induced pattern formation. It is well known that the Turing pattern owes its origin to the interplay of short-range activation and long-range diffusion of two interacting species. Choosing a homogeneous steady state in the absence of noise just outside the normal Turing domain amounts to allowing the dominance of the diffusive behavior over the kinetics of activation. The introduction of dichotomous noise now acts in two different ways. Since noise is multiplicative it is expected to induce a drift in the kinetics and therefore can effectively modify the local activation. On the other hand, the correlation between the noise and the system variables which appear as additional phase-space variables in the extended dynamics brings in modification of diffusion since the correlations take care of fluctuations beyond the mean-field limit. Therefore the presence of dichotomous noise with optimal strength and finite correlation time brings the local activation and long-range diffusion into an appropriate interacting condition where neither of these factors tend to overwhelm the other.

IV. DISCUSSION AND CONCLUSION

We have presented a general class of reaction-diffusion systems where a spatiotemporal instability can be induced by the application of dichotomous noise. The noise is characterized by zero mean and an exponential correlator. We have derived the bifurcation condition for noise-induced instability leading to stationary pattern formation, in the noise-strength–noise-correlation time parameter space for the dynamical state, which being above the normal Turing regime, remains homogeneously stable in the absence of noise. The general theoretical scheme has been applied to a CDIMA reaction-diffusion system. A major motivation behind such an application is the scope for experimental verification of the theoretical prediction, by stochastic modulation of a parameter of the model. The parameter of relevance is proportional to the ratio of the concentration of the two species, $[ClO_2]/[I_2]$. Earlier spectrophotometric analysis [39] shows that ClO_2 is a key species in the dynamics. It would seem natural that the concerned parameter can be stochastically modulated by controlling the flow of ClO_2, in the form $b \to b_0 + \xi(t)$ as required. Here $\xi(t)$ is the dichotomous noise with properties defined in Eq. (2.6). A possible design may be a CSTR-membrane reactor [24], which comprises a thin gel layer which lies on one wall of a CSTR which provides the continuous flow of reactants of the chlorine-dioxide-iodine-malonic acid system. With gel thickness of the order of 1/4 mm as demonstrated before [24], the diffusion time of the reactants into and out of the gel can be made very short (compared to the total residence time in the stirred flow reactor) which otherwise would be long for a standard open gel reactor, necessitating consideration of the details of flow processes involving gradients [40]. An advantage of such a design is that the concentration of feed chemicals for the reaction-diffusion process can be determined fairly accurately so that the dichotomous fluctuation of the concentration of ClO_2 can be controlled by varying the residence time (this is not to be confused with the residence time of a CSTR) of the two states of the noise. The diffusion time must also be short compared to the residence times of the two states of the noise. A CSTR-membrane reactor has been used previously in the study of Turing patterns [24]. The stochastic control of concentration of substrate was carried out earlier in experiments on glycolytic oscillations [25]. The role that dichotomous noise played in our study is different from the switching mechanism that operates between two different dynamical processes as investigated in earlier studies [16–20]. We now summarize the main conclusions of this study.

(i) The bifurcation condition and the associated numerical simulation reveal the existence of optimal strength and correlation time of dichotomous noise for noise-induced instability and pattern formation. Patterns disappear for very high and for very low values of noise strength. The optimal value of noise strength for a given correlation time is a reflection on the closeness of the time scales of the fluctuation of concentration and the deterministic dynamics of the chemical reaction.

(ii) An important element of the present formulation is that unlike the mean-field approaches, where the correlations are neglected, it takes care of the noise correlations by invoking the Furutzu-Novikov procedure for exponentially correlated random fluctuations in an appropriate way.

(iii) The analysis is a generalization of the linear stability analysis of the reaction-diffusion systems subjected to fluctuations of one of its parameters in an extended phase space. The additional phase-space variables appear as a result of the correlation between the system variables and the noise degree of freedom.

Our theoretical results on noise-induced instability are in good agreement with numerical simulations of the underlying CDIMA model which has played a key role in exploring many aspects of nonlinear chemical dynamics in spatially extended systems. We conclude by stressing that apart from activator-inhibitor dynamics the method can be easily implemented to other kinds of models in ecology and biology. The experimental verification of the theoretical predictions on pattern formation poses a challenge for ongoing research in this field.

ACKNOWLEDGMENT

Thanks are due to the Council of Scientific and Industrial Research, Government of India, for partial financial support.

[1] J. García-Ojalvo and J. M. Sancho, *Noise in Spatially Extended Systems* (Springer-Verlag, Berlin, 1999).

[2] F. Sagués, J. Sancho, and J. García-Ojalvo, Rev. Mod. Phys. **79**, 829 (2007).

[3] R. Benzi, A. Sutera, and A. Vulpiani, J. Phys. A: Math. Gen. **14**, L453 (1981); S. Fauve and F. Heslot, Phys. Lett. A **97**, 5 (1983); B. McNamara, K. Wiesenfeld, and R. Roy, Phys. Rev. Lett. **60**, 2626 (1988); L. Gammaitoni, P. Hänggi, P. Jung, and F. Marchesoni, Rev. Mod. Phys. **70**, 223 (1998).

[4] C. R. Doering and J. C. Gadoua, Phys. Rev. Lett. **69**, 2318 (1992).

[5] A. S. Pikovsky and J. Kurths, Phys. Rev. Lett. **78**, 775 (1997); Hu Gang, T. Ditzinger, C. Z. Ning, and H. Haken, *ibid.* **71**, 807 (1993).

[6] M. O. Magnasco, Phys. Rev. Lett. **71**, 1477 (1993); A. Parmeggiani, F. Julicher, A. Ajdari, and J. Prost, Phys. Rev. E **60**, 2127 (1999); C. R. Doering, W. Horsthemke, and J. Riordan, Phys. Rev. Lett. **72**, 2984 (1994); R. Bartussek, P. Reimann, and P. Hänggi, *ibid.* **76**, 1166 (1996); P. Reimann and T. C. Elston, *ibid.* **77**, 5328 (1996); T. Czernik, J. Kula, J. Łuczka, and P. Hänggi, Phys. Rev. E **55**, 4057 (1997); F. Marchesoni, *ibid.* **56**, 2492 (1997).

[7] D. Das, P. Ghosh, and D. S. Ray, J. Chem. Phys. **135**, 124104 (2011).

[8] W. Horsthemke and R. Lefever, *Noise-Induced Transitions: Theory and Applications in Physics, Chemistry, and Biology* (Springer-Verlag, Berlin, 1984).

[9] R. D. Astumian and M. Bier, Phys. Rev. Lett. **72**, 1766 (1994).

[10] D. Abbott and G. P. Harmer, Statist. Sci. **14**, 206 (1999); G. P. Harmer and D. Abbott, Nature (London) **402**, 864 (1999); J. M. R. Parrondo, G. P. Harmer, and D. Abbott, Phys. Rev. Lett. **85**, 5226 (2000).

[11] F. Lesmes, D. Hochberg, F. Morán, and J. Pérez-Mercader, Phys. Rev. Lett. **91**, 238301 (2003); G. Ahlersa, Physica D **51**, 421 (1991); T. Taneike, T. Nihei, and Y. Shiwa, Phys. Lett. A **303**, 212 (2002); J. García-Ojalvo, A. Hernández-Machado, and J. M. Sancho, Phys. Rev. Lett. **71**, 1542 (1993); Hou Zhonghuai, Yang Lingfa, Xiaobin Zuo, and Xin Houwen, *ibid.* **81**, 2854 (1998).

[12] P. S. Landa, A. A. Zaikin, and L. Schimansky-Geier, Chaos, Solitons Fractals **9**, 1367 (1998); A. Zaikin and J. Kurths, Chaos **11**, 570 (2001).

[13] C. Van den Broeck, J. M. R. Parrondo, J. Armero, and A. Hernández-Machado, Phys. Rev. E **49**, 2639 (1994).

[14] S. Dutta, S. S. Riaz, and D. S. Ray, Phys. Rev. E **71**, 036216 (2005); S. S. Riaz, S. Dutta, S. Kar, and D. S. Ray, Eur. Phys. J. B **47**, 255 (2005); S. S. Riaz, R. Sharma, S. P. Bhattacharyya, and D. S. Ray, J. Chem. Phys. **127**, 064503 (2007).

[15] P. C. Hohenberg and B. I. Halperin, Rev. Mod. Phys. **49**, 435 (1977); D. Forster, D. R. Nelson, and M. J. Stephen, Phys. Rev. A **16**, 732 (1977); P. Nozieres and F. Gallet, J. Physique (Paris) **48**, 353 (1987).

[16] J. Buceta, M. Ibañes, J. M. Sancho, and K. Lindenberg, Phys. Rev. E **67**, 021113 (2003).

[17] J. Buceta, K. Lindenberg, and J. M. R. Parrondo, Phys. Rev. Lett. **88**, 024103 (2001).

[18] J. Buceta, K. Lindenberg, and J. M. R. Parrondo, Phys. Rev. E **66**, 036216 (2002).

[19] J. Buceta and K. Lindenberg, Phys. Rev. E **66**, 046202 (2002).

[20] X. Sailer, D. Hennig, V. Beato, H. Engel, and L. Schimansky-Geier, Phys. Rev. E **73**, 056209 (2006).

[21] J. Buceta and K. Lindenberg, Phys. Rev. E **68**, 011103 (2003).

[22] J. Buceta and K. Lindenberg, Physica A **325**, 230 (2003).

[23] A. Sanz-Anchelergues, A. M. Zhabotinsky, I. R. Epstein, and A. P. Muñuzuri, Phys. Rev. E **63**, 056124 (2001).

[24] R. D. Vigil, Q. Ouyang, and H. L. Swinney, Physica A **188**, 17 (1992); see also B. Rudovics, E. Barillot, P. W. Davies, E. Dulos, J. Boissonade, and P. De Kepper, J. Phys. Chem. A **103**, 1790 (1999).

[25] S. Danø, P. G. Sørensen, and F. Hynne, Nature (London) **402**, 320 (1999); S. Kar and D. S. Ray, Phys. Rev. Lett. **90**, 238102 (2003).

[26] I. Lengyel and I. R. Epstein, Proc. Natl. Acad. Sci. USA **89**, 3977 (1992).

[27] I. Berenstein, L. Yang, M. Dolnik, A. M. Zhabotinsky, and I. R. Epstein, J. Phys. Chem. A **109**, 5382 (2005); M. Dolnik, A. M. Zhabotinsky, and I. R. Epstein, Phys. Rev. E **63**, 026101 (2001).

[28] I. Berenstein, A. P. Muñuzuri, L. Yang, M. Dolnik, A. M. Zhabotinsky, and I. R. Epstein, Phys. Rev. E **78**, 025101(R) (2008); P. Ghosh and D. S. Ray, J. Chem. Phys. **135**, 104112 (2011).

[29] I. Lengyel, S. Kádár, and I. R. Epstein, Phys. Rev. Lett. **69**, 2729 (1992); O. Jensen, V. O. Pannbacker, E. Mosekilde, G.

Dewel, and P. Borckmans, Phys. Rev. E **50**, 736 (1994); S. Setayeshgar and M. C. Cross, *ibid.* **58**, 4485 (1998); **59**, 4258 (1999).

[30] I. Berenstein, L. Yang, M. Dolnik, A. M. Zhabotinsky, and I. R. Epstein, Phys. Rev. Lett. **91**, 058302 (2003); I. Berenstein, M. Dolnik, L. Yang, A. M. Zhabotinsky, and I. R. Epstein, Phys. Rev. E **70**, 046219 (2004).

[31] S. Sen, P. Ghosh, and D. S. Ray, Phys. Rev. E **81**, 056207 (2010); S. Sen, P. Ghosh, S. S. Riaz, and D. S. Ray, *ibid.* **81**, 017101 (2010); **80**, 046212 (2009).

[32] A. K. Horváth, M. Dolnik, A. P. Muñuzuri, A. M. Zhabotinsky, and I. R. Epstein, Phys. Rev. Lett. **83**, 2950 (1999); P. Ghosh, S. Sen, S. S. Riaz, and D. S. Ray, Phys. Rev. E **79**, 056216 (2009).

[33] C. M. Topaz and A. J. Catllá, Phys. Rev. E **81**, 026213 (2010); S. Alonso and F. Sagués, *ibid.* **80**, 035203(R) (2009); D. G. Miguez, P. McGraw, A. P. Munuzuri, and M. Menzinger, *ibid.* **80**, 026208 (2009); A. Yadav, S. M. Milu, and W. Horsthemke, *ibid.* **78**, 026116 (2008).

[34] K. Furutsu, J. Res. Natl. Bur. Stand., Sect. D **67**, 303 (1963); E. A. Novikov, Sov. Phys. JETP **20**, 1290 (1965).

[35] Y. E. Shapiro and V. M. Logunov, Physica A **91**, 563 (1978).

[36] M. Gitterman, Phys. Rev. E **67**, 057103 (2003); J. Ray Chaudhuri, P. Chaudhury, and S. Chattopadhyay, J. Chem. Phys. **130**, 234109 (2009).

[37] J. D. Murray, *Mathematical Biology, I: An Introduction* (Springer, Berlin, 1989); F. R. Gantmacher, *The Theory of Matrices*, Vol. 2 (AMS Chelsea, Providence, 1959).

[38] D. Barik, P. K. Ghosh, and D. S. Ray, J. Stat. Mech. (2006) P03010.

[39] I. Lengyel, G. Rabai, and I. R. Epstein, J. Am. Chem. Soc. **112**, 4606 (1990); **112**, 9104 (1990).

[40] D. E. Strier, P. De Kepper, and J. Boissonade, J. Phys. Chem. A **109**, 1357 (2005).